Radiologic risk factors for mortality of patients with COVID-19 Pneumonia in Wuhan, China: a retrospective study

Xiang Li[1*], Zhen Chen[*], Ling Ye[*], Ling Zhang[*], Nannan Li, Dakai Jin, Liangxin Gao, Xinhui Liu, Bolin Lai, Jiawen Yao, Dazhou Guo, Hua Zhang, Le Lu, Jing Xiao, Lingyun Huang[#], Fen Ai[#], Xiang Wang[2#]

Summary

Background

Computed tomography (CT) characteristics associated with critical outcomes of patients with coronavirus disease 2019 (COVID-19) have been reported. However, CT risk factors for mortality are poorly understood. We aimed to investigate the automatically quantified CT imaging predictors for COVID-19 mortality.

Methods

In this retrospective study, laboratory-confirmed COVID-19 patients at Wuhan Central Hospital between December 9, 2019, and March 19, 2020, were included. A novel prognostic biomarker, V-HU score, depicting the volume of total pneumonia infection and the average Hounsfield unit (HU) value of consolidation areas was quantified from CT by an artificial intelligence (AI) system. Cox proportional hazards models were used to investigate risk factors for mortality.

Findings

This study included 238 patients (126 survivors and 112 non-survivors). The V-HU marker was an independent predictor (hazard ratio [HR] 2·78, 95% CI 1·50-5·17; p=0·0012) after adjusting for several COVID-19 prognostic indicators significant in univariable analysis. The prognostic performance of the model containing clinical and

[1] *Contributed equally.

[2] #Corresponding authors.

outpatient laboratory factors was improved by integrating the V-HU marker (c-index: 0·695 versus 0·728; p<0·0001). Older patients (age>=65 years; HR 3·56, 95% CI 1·64-7·71; p=0·0006) and younger patients (age<65 years; HR 4·60, 95% CI 1·92-10·99; p<0·0001) could be risk-stratified by the V-HU marker.

Interpretation

A combination of an increased volume of total pneumonia infection and high HU value of consolidation areas showed a strong correlation to COVID-19 mortality, as determined by AI quantified CT. The novel radiologic marker may be used for early risk assessment to prioritize critical care resources for patients at a high risk of mortality.

Funding

None.

Research in context

Evidence before this study

We searched PubMed for articles published up to Jul 21, 2020, using arbitrary combinations of the terms (“COVID”) AND ("prognosis" OR "prediction") AND (“mortality” OR "death"). Previous studies analyzed the risk factors of COVID-19 mortality using merely clinical and laboratory records. Only four articles demonstrated the value of quantitative CT in predicting the progression to critical illness, and one predicting the combined events of ICU admission/death. None of these studies explored the value of quantitative CT in direct predicting COVID-19 mortality. We aimed to develop a CT-based biomarker that enables automated quantitative risk stratification for COVID-19.

Added value of this study

In this retrospective cohort study of 238 patients from Wuhan Central Hospital, we developed an automated marker (V-HU) from CT imaging that integrated both the volume and density of the infected lung regions. Increased risk of COVID-19 death was associated with higher V-HU scores, irrespective of demographic factors (e.g., age), clinical factors (e.g., comorbidities), and laboratory parameters (e.g., blood oxygen). The multivariable survival model with the V-HU score improved the mortality prediction compared to that without the V-HU score in terms of c-index. The V-HU score could further stratify COVID-19 patients in the younger age group and the older age group into distinct prognostic groups.

Implications of all the available evidence

The automated quantitative V-HU score derived from CT by AI is an independent predictor of COVID-19 mortality. This assay is easy to perform, reproducible, and has the potential to be used for early risk assessment to prioritize critical care resources for patients at a high risk of mortality.

Introduction

The highly contagious coronavirus disease 2019 (COVID-19), broke up in 2019, has spread worldwide, posing a great threat to public health.[1] As of the 29th of June 2020, global coronavirus deaths have surpassed half a million, with the United States holding the highest death toll. As the confirmed cases and deaths dramatically increase, intensive-care units are nearly overwhelmed, and medical resources are of a dire shortage. In facing such a pandemic, finding out the risk factors associated with death and thus taking timely care towards those high-risk patients has the potential to reduce the mortality rate.

Currently, albeit the real-time reverse-transcriptase-polymerase-chain-reaction (RT-PCR) test is used as the gold standard for diagnosing COVID-19, it often suffers from the false negatives and longer turnaround times.[2] In the context of typical clinical presentation and exposure to other individuals with COVID-19, it may result in quarantine omission, acceleration of COVID-19 spread, consequently worsening the pandemic. It is critical to seek an accurate and efficient auxiliary screening and diagnosing method to identify high-risk patients of worse prognosis for prior treatment and early prevention in such an urgent situation. In many countries of Europe and Asia, CT imaging-based examination protocol stands out and becomes a complementary tool for the COVID-19 diagnosis with merits of high sensitivity to viral infection, easy access for patients, and quick acquisition of imaging.[3,4]

Following the COVID-19 pandemic spreading, research activities on COVID-19 have become very active. Epidemiological, clinical, laboratory and radiologic characteristics of COVID-19 are summarized in previous studies.[5-9] Clinical and laboratory risk factors for critical illness or death are also analyzed[6,10-13], where age is a well-recognized significant predictor in all studies, with additional clinical and laboratory factors or indices composed of multiple factors, such as d-dimer and SOFA score[10], MuLBSTA score[6], CD3+CD8+ T-cells and cardiac troponin levels[12], and deep-survival score involving neutrophil count and Lactate dehydrogenase[13]. On the other hand, several recent studies also demonstrate that chest CT imaging has great

prognostic value for COVID-19.[14-16] The volumes or volume ratios of lung infections, e.g., total lesion, or ground-glass opacity (GGO), are shown to be predictors of substantial outcomes (ICU admission and death).[14,15] However, no previous work has studied the direct correlation of quantitative CT features with the COVID-19 mortality in a patient cohort with a sufficient number of events.

In this study, we aim to investigate the CT based risk factors associated with COVID-19 mortality. The radiologic factors were automatically computed using the AI-based pulmonary imaging analysis system and validated with demographic, clinical, and laboratory risk factors.

Method

Study design and participants

In this retrospective study, patients diagnosed as COVID-19 in line with WHO interim guidance at Wuhan Central Hospital from December 9, 2019, to March 19, 2020, were enrolled.[17] Since large quantities of mildly ill patients did not come for further consultation, they were not included in this study owing to the absence of follow-up records. As a result, 244 patients met all the following inclusion criteria: (i) RT-PCR confirmed COVID-19; (ii) chest CT scanning at diagnosis time and revealing a typical ground glass shadow in lungs; (iii) with the final outcome (i.e., survival or dead) recorded (figure1). Among them, six patients lacked laboratory parameters were excluded. Ultimately, 238 patients with 238 CTs were enrolled. For the prognostic analysis, we defined the first CT examination time as the start point. The study was approved by the Research Ethics Commission of Wuhan Central Hospital, and the requirement for writing informed consent was waived by the Ethics Commission for the emergence of infectious diseases.

Data collection

We reviewed the clinical electronic medical records, nursing records, laboratory findings, and radiological examinations for all patients with COVID-19.

Epidemiological, demographic, clinical, laboratory and outcome data were extracted from electronic medical records using a standardized data collection form. All data were checked by two physicians (ZC and XL), and divergence between them can be adjudicated by a third senior expert (ZGX).

CT imaging protocol

CT scans at Wuhan Central Hospital were performed using GE BrightSpeed, Siemens SOMATOM Definition Flash, United Imaging uCT 760, and Philips iCT 256 scanners, respectively. These scans were conducted with the parameters of tube voltage 120 kV, tube current 50~250 mAs, pixel matrix 512x512. Most CT scans were reconstructed with a slice thickness of 1.0-1.5mm using sharp kernels.

CT image analysis

The whole lung field and the pneumonia infection regions were first segmented using a fully-automated AI-based pulmonary imaging analysis system.[18] A 2D UNet was trained to segment the lung field, and a 2·5D based deep learning model was developed to segment the pneumonia infection and pleural effusion regions using the UNet architecture[19] equipped with Resnet 34 backbone[20]. Then according to the Hounsfield unit (HU) values, the infection regions were further divided into GGO and consolidation by setting a threshold value.[21] Areas with HU values greater than -200 were regarded as consolidation, and areas with HU values between -700 and -200 were regarded as GGO. Network architectures for segmenting the whole lung field and pneumonia infection regions were illustrated in appendix figure S3 and figure S4, respectively.

CT imaging features were computed based on the size and density of the infection regions. Specifically, we calculated the infection volumes, the volume ratios (%) of the infection regions to the whole lung field, and the average HU values of the total pneumonia infection, GGO, consolidation, and the pleural effusion. Using these features, we further calculated a discrete V-HU score, as the proposed imaging biomarker, taking both the volume of total pneumonia infection (V) and the average HU value of the consolidation region (HU) into account. Specifically, the V-HU score was set to '0' (referring to the low-risk group) if both the V and the HU were less than

the corresponding median values in this population. Similarly, the V-HU score was set to ‘2’ (referring to the high-risk group) only if both the V and the HU were larger than the corresponding median values in this population. We set the V-HU score to ‘1’ (referring to the intermediate-risk group) for other conditions.

Statistical analysis

Continuous variables were expressed as median with interquartile range (IQR), and categorical variables were presented as the frequency with percentages (%). Differences between survivors and non-survivors were evaluated by the Mann-Whitney U test for continuous variables and the Chi-square test or Fisher's exact test for categorical variables as appropriate. A two-sided α of less than 0·05 was considered statistically significant.

Univariate and multivariate Cox proportional-hazards models were used to examine the association between the risk factors and patient outcomes. In-hospital death was assessed with four multivariate models under four different clinical circumstances: model 1 included all factors; model 2 (simulating outpatients without CT scans) included demographic, clinical, and outpatient laboratory factors; model 3 (simulating inpatients without CT scans) included demographic, clinical, both outpatient and inpatient laboratory factors; model 4 (simulating outpatients with CT scans) included demographic, clinical, outpatient laboratory and our radiologic marker. The selection of model covariates was detailed below.

For the missing laboratory parameters for which the overall deficiency rate was no more than 25%, we adopted a multivariate imputation approach, i.e. *aregImpute*[22]. By fitting flexible additive imputation models from non-missing data, target variables can be predicted through bootstrap resamples from a full Bayesian predictive distribution. Missing laboratory parameters including temperature (2 patients), white blood cell count (7 patients), neutrophil count (9 patients), lymphocyte count (7 patients), C-Reactive Protein (20 patients), blood oxygen (57 patients), d-dimer (56 patients), and lactic dehydrogenase (61 patients) were imputed. The data imputation process was carried out using the R package of '*Hmisc*' (v4·4·0).

Continuous variables were binarized by their corresponding median values as cutoffs. Significant variables (p-value < 0·05) in univariate analysis were considered as candidate variables for multivariate analysis. Considering the limited number of events, up to seven variables were chosen for the multivariate analysis to avoid overfitting in the models. The correlation between any two variables in the univariate analysis was illustrated in the appendix (figure S5). If there were several strongly correlated variables, only the most significant variable was included in the multivariate analysis. White blood cell count was not included in the model because of a strong correlation with the neutrophil count. For the correlated radiologic variables, only the most significant one, the V-HU score, was used in the multivariate analysis, since it considered both the volume and density of the pneumonia infection. Mortalities in the V-HU-defined subgroups were described using Kaplan-Meier analysis, and the log-rank test was used to assess whether the marker predicted mortality. All model-based results were presented with 95% confidence intervals.

All statistical analyses were conducted using Python 3·6 libraries unless otherwise indicated. We used functions that came with the DataFrame data structure in pandas (0·24·2) for calculating IQR and correlation matrices. Chi-square test and Mann-Whitney U test were done with scipy (1·3·0). Cox proportional hazards models and Kaplan-Meier curves were done with lifelines (0·24·6).

Results

The study cohort consisted of 238 COVID-19 patients. Demographic, clinical, and laboratory characteristics (obtained from outpatient and inpatient examinations) are reported in table 1. The median age of the patients was 65 years (IQR, 52-74). Non-survivors were older than those from survivors (p<0·0001). Non-survivors had a higher percentage of patients aged >75 years than the survivors (36% vs 10%). Male made up 58% of all patients but accounted for 68% of the non-survivors. Fever was a common symptom (72%) in all patients. Non-survivors had a higher prevalence of

cerebrovascular disease and hypertension than survivors, but not for cardiovascular disease and diabetes. For the laboratory parameters, a higher percentage of non-survivor than survivor presented with elevated levels of c-reactive protein, white blood cell count, neutrophil count, d-dimer, and lactic dehydrogenase.

The whole lung field and pneumonia infected regions from CT scans were automatically segmented and quantified using our pulmonary AI analysis system, of which the performance was shown in the appendix (table S1). Visualization of segmentation results was illustrated in the appendix (figure S1-S2, S6-S8). Quantified CT characteristics are summarized in table 2. Survivors had smaller absolute and percentage volumes of the total pneumonia infection as compared to non-survivors (263 ml vs 657 ml; 9% vs 22%; p<0·0001). Similar results were observed for the GGO and consolidation regions. The average HU value for the consolidation region was lower for survivors than that for non-survivors (-62 HU vs -51HU; p<0·0001). The average HU values for the total pneumonia infection and the GGO region did not show significant differences. The characteristics related to the pleural effusion region were similar between survivors and non-survivors.

Our new proposed radiologic marker, the V-HU score, was a strong univariable predictor of mortality. The score (0, 1, or 2) classified patients with COVID-19 pneumonia into three categories with respect to the risk of death: low risk; intermediate risk (HR for the comparison with low risk, 2·54; 95% CI 1·44-4·49); and high risk (HR for the comparison with low risk, 4·90; 95% CI 2·78-8·64) (figure 2). Age, sex, cerebrovascular disease, white blood cell count, neutrophil count, c-reactive protein, blood oxygen, lactic dehydrogenase, d-dimer, absolute and percentage volumes of the total pneumonia infection, GGO, consolidation, and average HU of consolidation and pleural effusion were also associated with death (table 3).

Table 4 shows the four multivariate Cox models for factors associated with death. In these models, older age and higher neutrophil count were associated with higher mortality. V-HU score was an independent predictor when it was included in multivariable models, i.e., HR=2·78 (95% CI 1·50-5·17; p=0·0012) in model 1 and HR=2·95 (95% CI 1·59-5·47; p=0·00059) in model 4. Compared to outpatient care of

model 2, adding the radiologic V-HU score (model 4) improved the mortality prediction (c-index: 0·728 [95% CI 0·687-0·781] vs 0·695 [95% CI 0·661-0·754]; p<0·0001). Furthermore, on the basis of inpatient examination parameters the addition of the V-HU score also improved the mortality prediction (c-index of model 1: 0·734 [95% CI 0·702-0·787] vs model 3: 0·716 [95% CI 0·682-0·768]; p<0·0001).

The V-HU score was a significant predictor of death in older patients (age>=65 years; for high vs low risk, HR 3·56, 95% CI 1·64-7·71; p=0·00060) and younger patients (age<65 years; for high vs low risk, HR 4·60, 95% CI 1·92-10·99; p<0·0001) subgroups. In the older patient group, both high and intermediate-risk patients characterized by the V-HU score presented poor prognosis with much lower survival rates than low-risk patients. In the younger patient group, high-risk patients still correlated with high COVID-19 mortality.

Discussion

In this retrospective study of confirmed COVID-19 patients, we identified that the increased mortality was independently associated with the following factors: (1) older age, (2) neutrophil count less than 3.6×10^9per L, and (3) higher V-HU score, which is a new radiologic biomarker integrating both the volume of pneumonia infections and density of consolidation calculated from CT images. The V-HU score can further stratify the risk in both younger (age < 65 years) and older (age >= 65 years) patients. Notably, the proposed V-HU score can be automatically computed by an adequately-evaluated AI-based pulmonary analysis system[18] and may produce fast, reliable, and reproducible prognostic measurement and evaluation in patients with COVID-19.

Previous studies have identified the volumes of different pneumonia infections as risk factors of patients with COVID-19 progressing to critical illness[14] or ICU admission/death[15]. The current study confirmed the correlation of increased infection volumes (total pneumonia infection, GGO, consolidation) and death in patients with COVID-19 in the univariate analysis. Moreover, we identified the importance of the

CT density in the pneumonia infection regions, particularly consolidation, and introduced a new comprehensive radiologic biomarker, V-HU score, that integrating both the density and volume of the pneumonia infections calculated from CT scans. The V-HU score is a strong prognostic factor of COVID-19 mortality in the univariate analysis and remained significant in the multivariate analysis. The pathophysiology analysis of deceased patients with COVID-19 shows that patients with higher intensity of the infection region have densely packed mucus between the small airways obstructing the airway's patency and its alveolar, where a large amount of viscous secretion overflows from the alveoli. Therefore, it inevitably reduces patients' gas exchange ventilation volume. As the density and volume of pneumonia infection increase, it is more likely to reduce patients' ventilation/blood flow ratio less than the critical point of 0·8. Then, insufficient oxygen between the alveoli and the pulmonary capillaries will result in the body's hypoxia and, thus, an increase in mortality.[23]

The V-HU score of 0, 1, 2 naturally categorized the patients into three groups: low, intermediate, and high-risk groups. From the Kaplan-Meier curve, the three groups have significantly different survival probabilities, which confirmed the high prognostic value of this radiologic biomarker. Moreover, the V-HU score can also identify patients at high risk of death in subgroups stratified by age. For example, in the age < 65 years subgroup, patients generally had a much lower mortality rate. However, those identified as high risk by the V-HU score may still require more intensive care to reduce the probability of their progression to death.

In this study, patients with older age, as confirmed in univariate and multivariate analyses, had a significantly increased risk of death. This is consistent with previous findings[10-12]. As elderly patients are often accompanied by a marked decline in cell-mediated immune function and humoral immune function[24], the propensity toward coagulation activation and impaired fibrinolysis, along with enhanced susceptibility to microbial mediators, contributes to the increased incidence of mortality in elderly patients. In addition, we also demonstrate that neutrophil count is a prognostic indicator of patients with COVID-19. The neutrophil count is strongly correlated with the white blood cell count. These two factors served as part of the first line of the innate immune

defense, played an important role in the immunopathology of COVID-19. With the exacerbation of the immune response, continuous infiltration of neutrophils at the site of infection produces exaggerated cytokines and chemokines that might result in the "cytokine storm" and contribute to the progression to poor prognosis during COVID-19[25]. Other clinical and laboratory factors have also been shown to predict COVID-19 mortality or critical outcomes in previous studies, such as d-dimer[10], lactate dehydrogenase[15], blood oxygen saturation, and C-reactive protein[14], and cardiovascular or cerebrovascular comorbidity[12].

However, these factors were not independently associated with death risk in our multivariate models, although lactate dehydrogenase showed prognostic value when this radiologic factor was not included.

Our fully automated AI-based pulmonary analysis system can provide the V-HU score within 15 seconds per CT scan on average, greatly shortening patients' waiting time and reducing radiologists' burden in the current COVID-19 pandemic. In contrast, it is almost impractical for radiologists to manually segment and identify different pneumonia infections to calculate this quantitative biomarker from 3D CT, considering the time and effort costs. Moreover, in situations that medical personnel and supplies are limited, such as emergency rooms, this CT-based V-HU score together with just patient age (or additionally easily accessed clinical factor, i.e., neutrophil count) can be used to quickly analyze the prognostic risk without further extra laboratory examinations reducing the burden for medical personnel.

Our study has several limitations. Firstly, this is a single-center study using retrospective data from Wuhan Central Hospital. It is unclear whether the strength of the association between the proposed radiologic marker and COVID-19 death differs in its prognostic implication across different populations. Second, not all patients had complete laboratory examinations leading to a certain amount of missing variables. Although we applied an interpolation approach that took all aspects of uncertainty in the imputations into account, this may still affect the role of some factors. Thirdly, patients enrolled during the early period of the pandemic faced the shortage of medical resources. The lacked timely antivirals, and inadequate treatment might also contribute

to the poor prognosis in some patients. Last but not least, in view of the absence of mildly ill patients' follow-up records, we did not include these patients in our analysis, which to some extent, might lead to a higher mortality rate reported in this study.

To our best knowledge, we conduct an imaging-based retrospective prognosis study of the COVID-19 mortality using the largest number of non-survivors to date. We propose a new CT-based radiologic imaging biomarker, V-HU score, integrating the volume and density of the infected lung regions, and showing that it is an independent and strong predictor of death in patients with COVID-19. The V-HU score can be automatically and reliably computed from CT images by the AI algorithm. When combining it with age and neutrophil count, good prognostic performance has been achieved.

Contributors

LYH, FA, XW, XL, ZC, LY and LZ had the idea for and designed the study and had full access to all of the data in the study and take responsibility for the integrity of the data and the accuracy of the data analysis. LXG, XHL, NNL, LY and LYH designed the AI system for CT image characteristics quantification in this study. NNL, LZ, DKJ and LY drafted the paper. XHL, BLL, LY, LZ, JWY and NNL did the statistical analysis, and all authors critically revised the manuscript for important intellectual content and gave final approval for the version to be published. HZ, ZC, XL, BLL and LYH collected the data. All authors agree to be accountable for all aspects of the work in ensuring that questions related to the accuracy or integrity of any part of the work are appropriately investigated and resolved.

Declaration of interests

We declare no competing interests.

Data sharing

After publication, the data will be made available to others on reasonable requests to the corresponding author. A proposal with detailed description of study objectives and statistical analysis plan will be needed for evaluation of the reasonability of requests. Additional materials might also be required during the process of evaluation. Deidentified participant data will be provided after approval from the corresponding author and Wuhan Jin Yin-tan Hospital.

Acknowledgments

We thank all patients and their families involved in the study.

References

[1] Zhu N, Zhang D, Wang W, et al. A novel coronavirus from patients with pneumonia in China, 2019. *N Engl J Med* 2020; published online Jan 24. DOI:10.1056/NEJMoa2001017.

[2] Xie X, Zhong Z, Zhao W, et al. Chest CT for typical 2019-nCoV pneumonia: relationship to negative RT-PCR testing. *Radiology* 2020; Published online Feb 12. DOI: 10.1148/radiol.2020200343.

[3] Ai T, Yang Z, Hou H, et al. Correlation of chest CT and RT-PCR testing in coronavirus disease 2019 (COVID-19) in China: a report of 1014 cases. *Radiology* 2020; Published online Feb 26. DOI: 10.1148/radiol.2020200642.

[4] Prokop M, van Everdingen W, van Rees Vellinga T, et al. CO-RADS–A categorical CT assessment scheme for patients with suspected COVID-19: definition and evaluation. *Radiology* 2020; Published online 2020 Apr 27. DOI: 10.1148/radiol.2020201473.

[5] Guan, Wei-jie, et al. Clinical characteristics of coronavirus disease 2019 in China. *N Engl J Med* 2020; **382**: 1708–1720.

[6] Chen, Nanshan, et al. Epidemiological and clinical characteristics of 99 cases of 2019 novel coronavirus pneumonia in Wuhan, China: a descriptive study. *Lancet* 2020; **395**: 507–513.

[7] Huang C, Wang Y, Li X, et al. Clinical features of patients infected with 2019 novel coronavirus in Wuhan, China. *Lancet* 2020; **395**: 497–506.

[8] Wang, Dawei, et al. Clinical characteristics of 138 hospitalized patients with 2019 novel coronavirus–infected pneumonia in Wuhan, China. *JAMA* 2020; **323**: 1061-–1069.

[9] Feng Y, Ling Y, Bai T, et al. COVID-19 with different severities: a multicenter study of clinical features. *Am J Respir Crit Care Med* 2020; **201**: 1380-1388.

[10] Zhou, Fei, et al. Clinical course and risk factors for mortality of adult inpatients with COVID-19 in Wuhan, China: a retrospective cohort study. *Lancet* 2020; **8**: 475–481.

[11] Yang, Xiaobo, et al. Clinical course and outcomes of critically ill patients with SARS-CoV-2 pneumonia in Wuhan, China: a single-centered, retrospective, observational study. *LANCET RESP MED* 2020; **8**: 475–481.

[12] Du R H, Liang L R, Yang C Q, et al. Predictors of mortality for patients with COVID-19 pneumonia caused by SARS-CoV-2: a prospective cohort study. *EUR RESPIR J* 2020; **55**: 2000524.

[13] Liang, Wenhua, et al. Early triage of critically ill COVID-19 patients using deep learning. *Nat Commun* 2020; **11**: 1–7.

[14] Zhang K, Liu X, Shen J, et al. Clinically applicable AI system for accurate diagnosis, quantitative measurements, and prognosis of covid-19 pneumonia using computed tomography. *Cell* 2020; **181**: 1423–1433.

[15] Colombi D, Bodini F C, Petrini M, et al. Well-aerated lung on admitting chest CT to predict adverse outcome in COVID-19 pneumonia. *Radiology* 2020 Published online Apr 17. DOI: 10.1148/radiol.2020201433.

[16] Yuan M, Yin W, Tao Z, et al. Association of radiologic findings with mortality of patients infected with 2019 novel coronavirus in Wuhan, China. *PloS one,* 2020; **15**: e0230548.

[17] WHO. Clinical management of severe acute respiratory infection when novel coronavirus (nCoV) infection is suspected. Jan 11, 2020. https://www.who.int/publications-detail/clinical-management-ofsevere-acute-respiratory-infection-when-novel-coronavirus-(ncov)infection-is-suspected (accessed Jul 23, 2020).

[18] Li Z, Zhong Z, Li Y, et al. From Community Acquired Pneumonia to COVID-19: A Deep Learning Based Method for Quantitative Analysis of COVID-19 on thick-section CT Scans. *ER* 2020; Published online Jul 18. DOI: https://doi.org/10.1007/s00330-020-07042-x.

[19] Ronneberger O, Fischer P, Brox T. U-net: Convolutional networks for biomedical image segmentation. *International Conference on Medical image computing and computer-assisted intervention* 2015: 234-241.

[20] He K, Zhang X, Ren S, et al. Deep residual learning for image recognition. *In Proceedings of the IEEE conference on computer vision and pattern recognition* 2016: 770-778.

[21] Okada T, Iwano S, Ishigaki T, et al. Computer-aided diagnosis of lung cancer: definition and detection of ground-glass opacity type of nodules by high-resolution computed tomography. *JPN J RADIOL* 2009; **27**: 91–99.

[22] Donders A, Van Der Heijden, Stijnen T, et al. A gentle introduction to imputation of missing values. *J Clin Epidemiol* 2006; **59**: 1087-1091.

[23] Schaefer I M, Padera R F, Solomon I H, et al. In situ detection of SARS-CoV-2 in lungs and airways of patients with COVID-19. *Mod Pathol* 2020*;* 1–11.

[24] Opal S M, Girard T D, Ely E W. The immunopathogenesis of sepsis in elderly patients. *Clin Infect Dis* 2005, **41**: S504–S512.

[25] Tomar B, Anders H J, Desai J, et al. Neutrophils and Neutrophil Extracellular Traps Drive Necroinflammation in COVID-19. *Cells* 2020; **9**(6): 1383.

Figure legends

Figure 1: Diagram showing the patient selection process. COVID-19=Coronavirus Disease 2019. CT=computed tomography.

Figure 2: Kaplan-Meier estimates of survival probability as a function of the number of patients at risk segregated by the V-HU score.
Note: As some patients in the intermediate-risk and the high-risk group died on the day of their first CT examination, their curves did not start from 1·0.

Figure 3: Kaplan-Meier estimates of survival probability of patients in >=65 years group and <65 years group with COVID-19 as a function of the number of patients at risk segregated by V-HU score.
Note: As some patients in the intermediate-risk and the high-risk group died on the day of their first CT examination, their curves did not start from 1·0.

Table 1: Demographic, clinical and laboratory characteristics of 238 COVID-19 patients

	ALL (n=238)	Survivor (n=126)	Non-Survivor (n=112)	p value
Demographics and clinical characteristics				
Age (years)	64·50 (51·25-74·00)	57·00 (37·00-68·00)	69·50 (63·00-80·25)	<0·0001
<=40	43/238 (18%)	42/126 (33%)	1/112 (89%)	<0·0001
40-65	83/238 (35%)	47/126 (37%)	36/112 (32%)	
65-75	59/238 (25%)	24/126 (19%)	35/112 (31%)	
>75	53/238 (22%)	13/126 (10%)	40/112 (36%)	
Sex				
Male	102/238 (43%)	67/126 (53%)	35/112 (31%)	0·00060
Female	136/238 (57%)	59/126 (47%)	77/112 (69%)	
Temperature	37·90 (37·20-38·50)	38·00 (37·40-38·60)	37·80 (37·10-38·20)	0·028
Fever (>=37·3)	171/236 (72%)	97/126 (77%)	74/110 (67%)	0·096
Comorbidity	150/238 (63%)	68/126 (54%)	82/112 (73%)	0·0021
Cardiovascular disease	42/238 (18%)	17/126 (13%)	25/112 (22%)	0·075
Hypertension	87/238 (37%)	38/126 (30%)	49/112 (44%)	0·030
Cerebrovascular disease	23/238 (10%)	3/126 (2·4%)	20/112 (18%)	<0·0001
Diabetes	46/238 (19%)	21/126 (17%)	25/112 (22%)	0·27
Others	65/238 (27%)	33/126 (26%)	32/112 (29%)	0·68
Outpatient laboratory parameters				
White blood cell count ($\times 10^9$ per L)	5·90 (4·32-8·02)	5·14 (3·90-6·65)	7·01 (5·21-9·22)	<0·0001
<=4	49/231 (21%)	33/122 (27%)	16/109 (15%)	<0·0001
4-10	151/231 (65%)	82/122 (67%)	69/109 (63%)	
>10	31/231 (13%)	7/122 (5·7%)	24/109 (22%)	
Neutrophil count ($\times 10^9$ per L)	4·53 (2·97-7·87)	3·59 (2·63-5·87)	6·43 (3·85-9·26)	<0·0001
<=3·6	84/229 (37%)	61/121 (50%)	23/108 (21%)	<0·0001
>3·6	145/229 (0·63)	60/121 (50%)	85/108 (79%)	
lymphocyte count ($\times 10^9$ per L)	0·79 (0·53-1·06)	0·85 (0·62-1·22)	0·70 (0·49-0·95)	0·00050
<=0·8	118/231 (51%)	55/122 (45%)	63/109 (58%)	0·054
>0·8	113/231 (49%)	67/122 (55%)	46/109 (42%)	
C-Reactive Protein (mg/L)	3·84 (1·45-7·83)	2·29 (0·59-6·08)	5·40 (3·06-10·71)	<0·0001
<=1	44/218 (20%)	38/118 (32%)	6/100 (6·0%)	<0·0001
>1	174/218 (80%)	80/118 (68%)	94/100 (94%)	
Inpatient laboratory parameters				
Blood Oxygen	60·00 (49·00-80·00)	68·50 (56·50-87·00)	56·00 (45·50-73·50)	0·00060
<=80	136/181 (75%)	57/86 (66%)	79/95 (83%)	0·0087

>80	45/181 (25%)	29/86 (34%)	16/95 (17%)	
D-dimer (μg/L)	2·23 (0·73-7·70)	1·11 (0·57-4·65)	4·67 (1·40-9·32)	<0·0001
<=0·5	23/182 (13%)	20/95 (21%)	3/87 (3·0%)	<0·0001
0·5-1	35/182 (19%)	25/95 (26%)	10/87 (11%)	
>1	124/182 (68%)	50/95 (53%)	74/87 (85%)	
lactic dehydrogenase (U/L)	316·00 (214·00-450·00)	244·00 (187·00-350·00)	406·50 (263·75-576·75)	<0·0001
<=245	64/177 (36%)	45/89 (51%)	19/88 (22%)	<0·0001
>245	113/177 (64%)	44/89 (49%)	69/88 (78%)	

Data are median (IQR), n (%), or n/N (%). p values were calculated by Mann-Whitney U test, Chi-square test, or Fisher's exact test, as appropriate.

Table 2: CT quantification indexes of 238 COVID-19 patients

	ALL (n=238)	Survivor (n=126)	Non-Survivor (n=112)	p value
Total pneumonia infection				
Volume of total pneumonia infection (ml)	437·71 (141·52-1124·64)	263·41 (67·98-746·25)	657·70 (306·50-1410·11)	<0·0001
Ratio of total pneumonia infection (%)	15·94 (3·96-42·24)	9·09 (1·56-37·19)	21·78 (9·03-50·10)	<0·0001
HU of total pneumonia infection	-501·12 (-571·26-419·82)	-494·85 (-559·65-434·01)	-515·06 (-572·66-407·77)	0·62
GGO				
Volume of GGO (ml)	219·62 (77·04-604·84)	156·15 (37·71-458·80)	335·56 (150·08-809·13)	<0·0001
Ratio of GGO (%)	8·05 (2·12-23·74)	4·95 (1·02-20·48)	11·38 (4·28-27·05)	0·00030
HU of GGO	-486·07 (-514·43-463·90)	-484·69 (-513·76-462·69)	-491·85 (-518·09-464·10)	0·58
Consolidation				
Volume of consolidation(ml)	61·08 (17·78-161·00)	42·89 (9·21-133·59)	95·80 (29·95-210·75)	0·00070
Ratio of consolidation (%)	2·14 (0·53-6·91)	1·31 (0·32-5·61)	2·75 (0·82-7·52)	0·0039
HU of consolidation	-55·45 (-71·70-43·52)	-62·07 (-74·26-50·09)	-51·05 (-64·71-39·24)	0·00015
Pleural Effusion				
Volume of pleural effusion (ml)	0·00 (0·00-0·00)	0·00 (0·00-0·00)	0·00 (0·00-0·00)	0·036
Ratio of pleural effusion (%)	0·00 (0·00-0·00)	0·00 (0·00-0·00)	0·00 (0·00-0·00)	0·038
HU of pleural effusion	8·98 (4·62-23·10)	4·31 (2·12-5·07)	20·86 (7·34-24·72)	0·043
Volume of pleural effusion* (ml)	13·61 (96·95)	6·89 (52·88)	21·17 (129·66)	0·036

Data are median (IQR), n (%), or n/N (%). p values were calculated by Mann-Whitney U test, Chi-square test, or Fisher's exact test, as appropriate. GGO = ground-glass opacity. Since the number of patients with pleural effusion were too small, both median and IQR of pleural effusion volume were 0·00. In order to better explore the association between pleural effusion and patients with COVID-19, we also showed the mean value and standard deviation of pleural effusion volume in the row "V-PE* (ml)".

Table 3: Results from univariate cox proportional hazards regression in 238 patients with COVID-19

	Hazard Ratio (95% CI)	p value
Demographics and clinical characteristics		
Age (years)		
>=65	3·36 (2·22-5·07)	<0·0001
<65	1 (ref)	··
Sex		
Male	1·84 (1·23-2·75)	0·0030
Female	1 (ref)	··
Temperature		
>=37·90	0·74 (0·51-1·07)	0·11
<37·90	1 (ref)	··
Comorbidity present (vs not present)		
Cerebrovascular disease	2·29 (1·36-3·85)	0·0020
Cardiovascular disease	1·41 (0·91-2·21)	0·13
Diabetes	1·37 (0·88-2·13)	0·17
Hypertension	1·43 (0·98-2·07)	0·062
Outpatient laboratory parameters		
White blood cell count ($\times 10^9$ per L)		
>=5·90	2·46 (1·67-3·64)	<0·0001
<5·90	1 (ref)	··
Neutrophil count ($\times 10^9$ per L)		
>=4·53	2·66 (1·80-3·94)	<0·0001
<4·53	1 (ref)	··
Lymphocyte count ($\times 10^9$ per L)		
>=0·79	0·70 (0·48-1·02)	0·061
<0·79	1 (ref)	··
C-Reactive Protein (mg/L)		

>=3·84	1·88 (1·29-2·74)	0·0010
<3·84	1 (ref)	··
Inpatient laboratory parameters		
Blood oxygen		
>=60·00	0·54 (0·37-0·79)	0·0010
<60·00	1 (ref)	··
D-dimer (μg/L)		
>=2·23	1·75 (1·20-2·55)	0·0040
<2·23	1 (ref)	··
Lactic dehydrogenase (U/L)		
>=316·00	2·30 (1·58-3·37)	<0·0001
<316·00	1 (ref)	··
Radiologic parameters		
volume of total pneumonia infection (ml)		
>=437·71	2·81 (1·89-4·17)	<0·0001
<437·71	1 (ref)	··
HU of total pneumonia infection		
>=-501·12	0·88 (0·61-1·28)	0·50
<-501·12	1 (ref)	··
Ratio of total pneumonia infection (%)		
>=15·94	2·26 (1·54-3·32)	<0·0001
<15·94	1 (ref)	··
volume of GGO (ml)		
>=219·62	2·26 (1·54-3·32)	<0·0001
<219·62	1 (ref)	··
HU of GGO		
>=-486·07	0·75 (0·52-1·09)	0·14
<-486·07	1 (ref)	··
ratio of GGO (%)		
>=8·05	2·25 (1·53-3·32)	<0·0001
<8·05	1 (ref)	··

volume of consolidation (ml)		
>=61·08	2·18 (1·48-3·19)	<0·0001
<61·08	1 (ref)	··
HU of consolidation		
>=-55·45	2·05 (1·40-3·01)	0·00023
<-55·45	1 (ref)	··
ratio of consolidation (%)		
>=2·14	1·70 (1·17- 2·47)	0·0060
<2·14	1 (ref)	··
volume of pleural effusion (ml)		
>=0·00	1·93 (1·03-3·60)	0·039
<0·00	1 (ref)	··
HU of pleural effusion		
>=8·98	7·42 (1·52-36·11)	0·013
<8·98	1 (ref)	··
ratio of pleural effusion (%)		
>=0·00	1·93 (1·03-3·60)	0·039
<0·00	1 (ref)	··
V-HU		
0·00	1 (ref)	··
1·00	2·54 (1·44-4·49)	<0·0001
2·00	4·90 (2·78-8·64)	<0·0001

The V-HU score was our new proposed CT biomarker, which took both the volume of total pneumonia infection and the average HU value of consolidation into account. The V-HU score was '0' (categorized into low-risk group) if both the volume of total pneumonia infection and the average HU value of the consolidation region were less than the corresponding median values in this population. Similarly, the V-HU score was '2' (categorized into high-risk group) only if both the volume of total pneumonia infection and the average HU value of the consolidation region were more than the corresponding median values in this population. Other conditions were assigned to the value of '1' (categorized into intermediate-risk group).

Table 4: Results from multivariate cox proportional hazards regression in 238 patients with COVID-19

	Model 1		Model 2		Model 3		Model 4	
	Hazard Ratio (95% CI)	**p value**	**Hazard Ratio** (95% CI)	**p value**	**Hazard Ratio** (95% CI)	**p value**	**Hazard Ratio** (95% CI)	**p value**
demographic/clinical variables								
Age (years)								
>=65	2·59 (1·67-4·03)	<0·0001	3·03 (1·97-4·68)	<0·0001	2·83 (1·82-4·39)	<0·0001	2·69 (1·74-4·17)	<0·0001
<65	1 (ref)	··	1 (ref)	··	1 (ref)	··	1 (ref)	··
Sex								
Male	··	··	1·39	0·12	1·30	0·22	1·30	0·23
Female			1 (ref)	··	1 (ref)	··	1 (ref)	··
Cerebrovascular disease (vs not present)	0·87 (0·50-1·51)	0·62	0·86 (0·50-1·48)	0·59	0·94 (0·55-1·62)	0·83	0·76 (0·44-1·32)	0·33
outpatient laboratory variables								
Neutrophil count ($\times$ 10^9per L)								
>=4·53	1·82 (1·19-2·79)	0·0060	2·09 (1·37-3·18)	0·00060	1·93 (1·26-2·95)	0·0026	1·93 (1·27-2·94)	0·00020
<4·53	1 (ref)	··	1 (ref)	··	1 (ref)	··	1 (ref)	··
C-Reactive Protein (mg/L)								
>=3·84	1·19 (0·77-1·82)	0·43	1·45 (0·96-2·18)	0·079	1·22 (0·79-1·88)	0·37	1·32 (0·87-2·00)	0·19
>=3·84	1 (ref)	··	1 (ref)	··	1 (ref)	··	1 (ref)	··
Inpatient laboratory parameters								
Blood Oxygen								
>=60·00	0·81 (0·54-1·20)	0·29	··	··	0·81 (0·55-1·21)	0·31	··	··
<60·00	1 (ref)	··	··	··	1 (ref)	··	··	··
Lactic dehydrogenase								
>=316·00	1·52 (0·93-2·50)	0·094	··	··	1·66 (1·01-2·71)	0·044	··	··
<316·00	1 (ref)	··	··	··	1 (ref)	··	··	··
Radiologic variables								
V-HU								
0·00	1 (ref)	··	··	··	··	··	1 (ref)	··
1·00	1·62 (0·90-2·92)	0·11	··	··	··	··	1·64 (0·91-2·96)	0·10

2·00	2·78 (1·50-5·17)	0·0012	··	··	··	··	2·95 (1·59-5·47)	0·00059
C-index	0·734 (0·702-0·787)	··	0·695 (0·661-0·754)	··	0·716 (0·682-0·768)	··	0·728 (0·687-0·781)	··

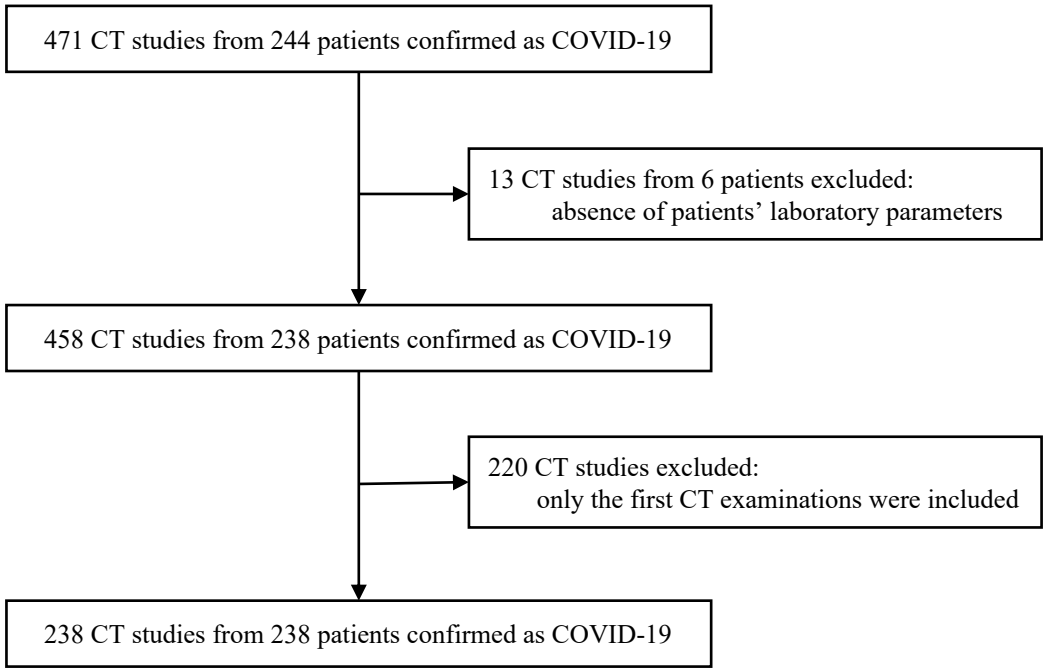

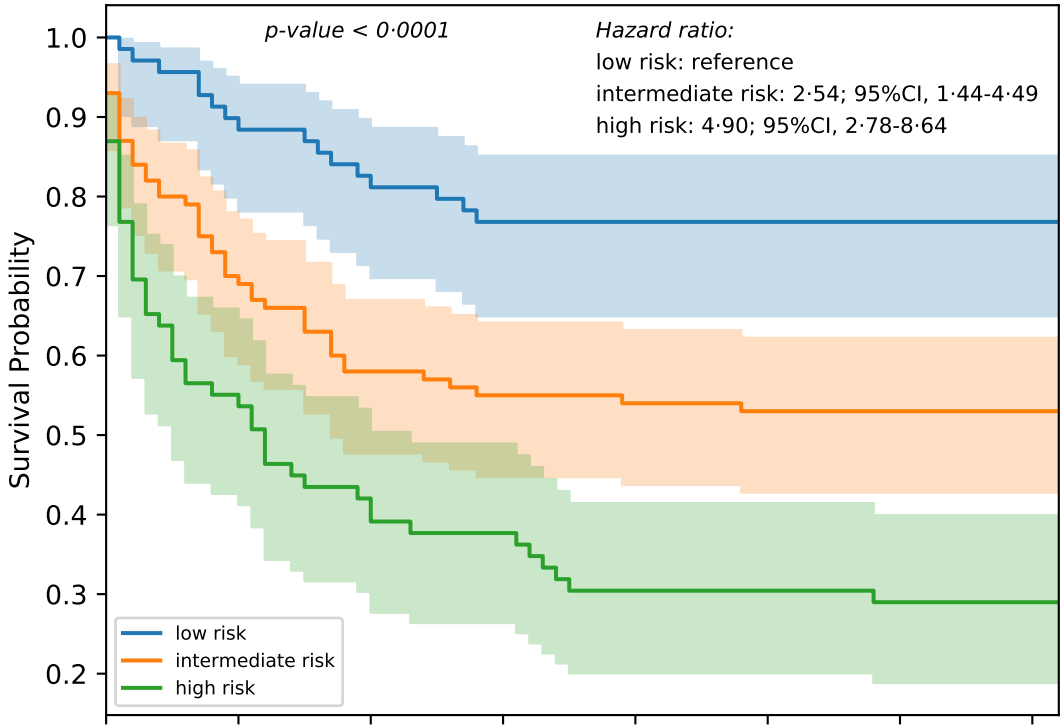

Numbers at low risk	69	61	56	53	53	53	53	53
Numbers at intermediate risk	100	69	58	55	53	53	53	53
Numbers at high risk	69	37	27	26	21	21	20	20

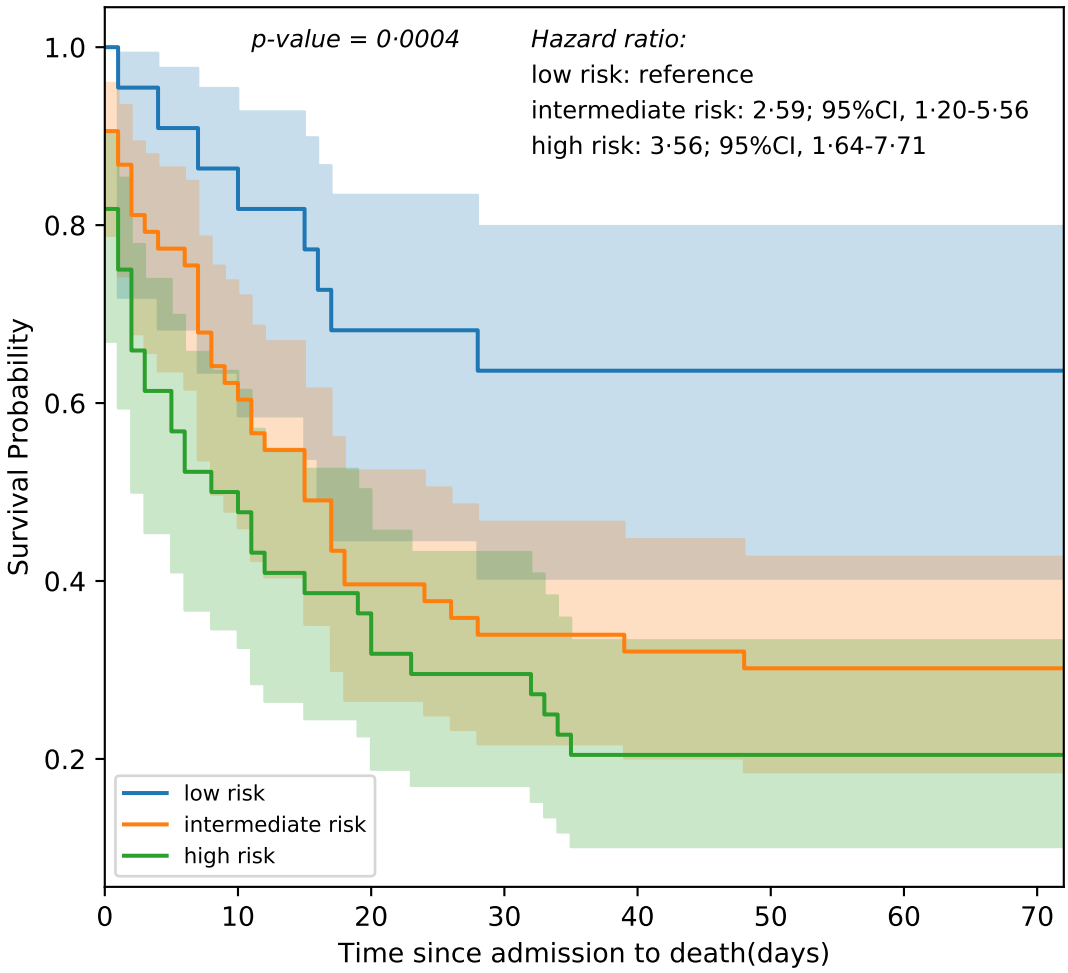

Numbers at low risk	22	18	15	14	14	14	14	14
Numbers at intermediate risk	53	32	21	18	17	16	16	15
Numbers at high risk	44	21	14	13	9	9	9	9

(a) >=65 years group

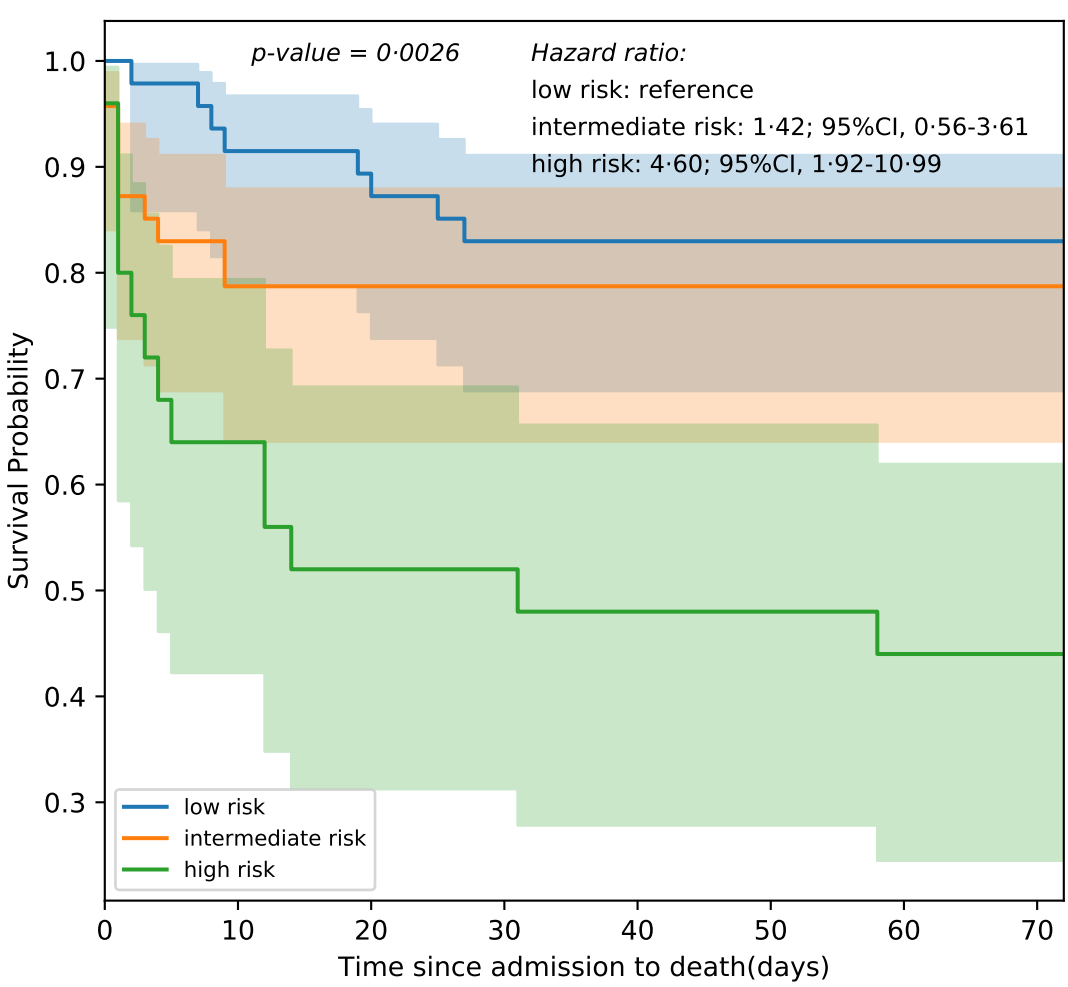

Numbers at low risk	47	43	41	39	39	39	39	39
Numbers at intermediate risk	47	37	37	37	37	37	37	37
Numbers at high risk	25	16	13	13	12	12	11	11

(b) <65 years group